Multi-Band Acoustic-Wave-Lumped-Element Resonator-Based Bandstop Filters With Continuously Tunable Stopband Bandwidths

Dimitra Psychogiou and Dakotah J. Simpson
University of Colorado at Boulder, Boulder, CO 80309, USA

***Abstract*—A new class of multi-band acoustic-wave-lumped-element-resonator (AWLR)-based bandstop filters (BSFs) is reported. It is based on *N* multi-resonant AWLRs—shaped by *K* AWLRs and 2*K* inverters—that are connected to an all-pass network and result in *K N*th order rejection bands. The proposed concept allows the realization of multiple rejection bands with the following characteristics: i) fractional bandwidths (FBWs) larger than the electromechanical coupling coefficient k_t^2 of its constituent acoustic-wave resonators, ii) continuously variable and independently-controlled FBWs, iii) intrinsically-switched stopbands, and iv) an all pass state. For proof-of-concept validation purposes a dual-band prototype was designed, built, and tested. It exhibits two stopbands centered at 418 and 433 MHz that can be continuously-tuned in FBW (up to 7.7:1 tuning range) and in number.**

***Index Terms*— Acoustic-wave (AW) filter, bandstop filter (BPF), high-quality-factor (*Q*) filter, k_t^2 enhancement, RF/microwave filter, surface acoustic-wave (SAW) resonator.**

I. Introduction

The rapid growth of wireless communication systems is increasingly calling for reconfigurable RF transceivers with interference suppression capabilities [1]. This is particularly critical for the ones located in the UHF band (300-3000 MHz) due to the large number of co-located RF sources at these frequencies that result in multiple interfering signals with variable frequency and bandwidth (BW) and desensitize their RF receivers.

Bandstop filters (BSFs) with small physical size, reconfigurable response, and large levels of attenuation have been identified as key elements for the preselect stages of the front-ends of these systems. However, their realization remains a great challenge due to the lack of resonators that are simultaneously tunable, small, and exhibit high-quality factor (*Q*). Although acoustic-wave-resonator (AWR)-based RF filters—i.e., surface acoustic-wave (SAW), bulk acoustic-wave (BAW)— have been the key filtering technology of communication transceivers, the majority of them exhibit bandpass response, fractional bandwidth (FBW) smaller than the electromechanical coupling coefficient (FBW< 0.4-0.8k_t^2 [2]), and are mostly static which inhibits their suitability for multi-interference suppression.

A small number of BSFs using AWRs have been reported in the open technical literature, as for example the ones in [3]-[8]. Nevertheless, they are only able to suppress a single band, they exhibit static response with FBW <k_t^2, and suffer from increased levels of loss in their passband areas. In an alternative approach [5], [6], AWRs are effectively combined with lumped-elements (LEs) to increase the passband FBW (FBW: 1-5k_t^2) above k_t^2 as well as to allow for continuous BW tuning by incorporating variable reactive elements in the BSF's inverters [7]. However, this concept only allows the realization of a single band.

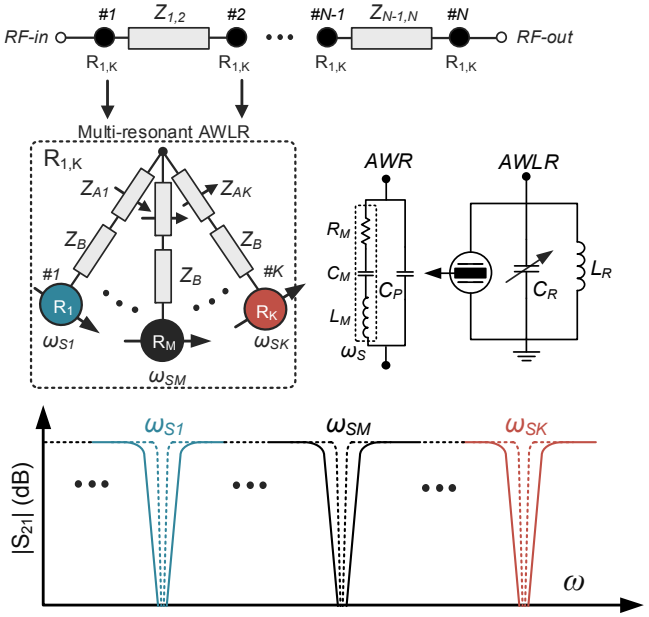

Fig. 1. Block diagram and conceptual transfer function of the multi-band AWLR-based BSF that exhibits *K* stopbands (centered at ω_{SI}, ω_{SK}), each one shaped by *N* TZs. $Z_{1,2}$, $Z_{N,N-1}$, Z_{AK}, Z_B: impedance inverters, R_1, R_K: AWLRs.

Taking into consideration the aforementioned shortcomings, a new class of multi-band acoustic-wave-lumped-element-resonator (AWLR)-based BSFs is reported. They exhibit the following characteristics: i) multiple enhanced-FBW stopbands, ii) continuously-variable and independently-controlled stopband BWs, iii) intrinsically-switched rejection bands, and iv) an all-pass state. The content of this paper is organized as follows. In Section II, the multi-band AWLR-based BSF concept is presented. Section III reports on its experimental validation. Finally, a summary of the relevant contributions of this work is given in Section IV.

II. Theoretical Foundations

The circuit details and conceptual transfer function of the multi-band (*K* stopbands) AWLR-based BSF are illustrated in Fig. 1. It is based on *N* multi-resonant AWLRs ($R_{1,K}$)—shaped by *K* AWLRs and 2*K* inverters—that are connected to an all-pass network—shaped by $Z_{1,2}$-$Z_{N-1,N}$—and result in *K N*th order rejection bands. Each $R_{1,K}$ is made from *K* AWLRs (R_1-R_K) and

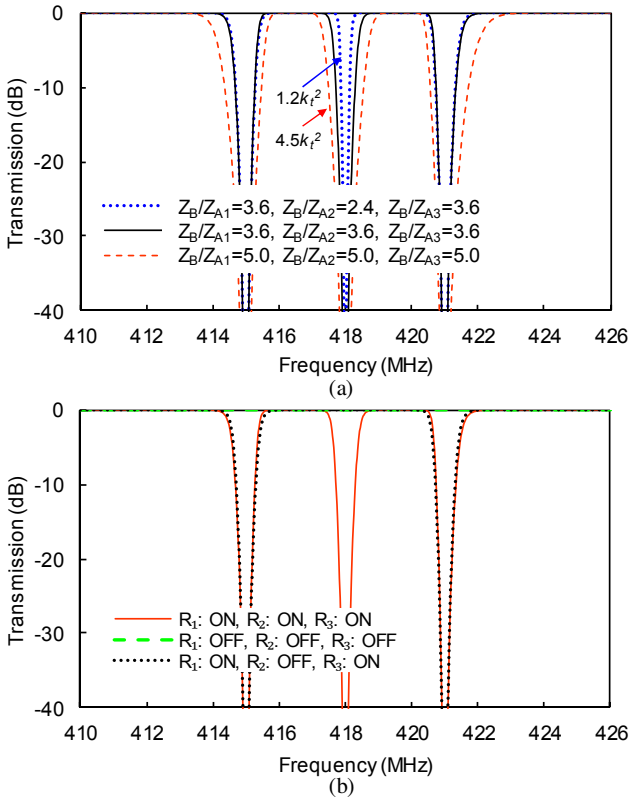

Fig. 2. (a) Theoretical power transmission response of a third-order tri-band AWLR-based BSF (K=3, N=3) for various levels of Z_B/Z_{AK}. (b) Theoretical power transmission response of a third-order tri-band AWLR-based BSF (K=3, N=3) for different number of activated branches (through ideal switches at the interconnection point between $Z_{1,2}$ /$Z_{2,1}$ and Z_A). The rest of the circuit parameters are: AWRs with k_t^2= 0.08 %, (L_M= 90 µH, Q= ∞), Z_{12}=Z_{23}= 1.414, Z_A=1. All impedances are normalized to the system impedance Z_0= 50 Ω.

each AWLR comprises one AWR—motional capacitance: C_M, inductance: L_M, resistance: R_M, parallel capacitance: C_P, series resonant frequency: ω_S, and anti-resonant frequency: ω_A—and one LE resonator (C_R, L_R). The center frequency of each band is set by the series resonant frequency ω_{SK} of the AWR and the resonant frequency ω_R of the LE resonator that is shaped by C_P, L_R, C_R is set equal to ω_{SK} in order for a single high-Q resonance—decoupled from the ω_A of the AWR—to be realized at ω_{SK}. Each AWLR is connected to the all-pass network through two sets of impedance inverters Z_{AK}, Z_B, that control the FBW of each stopband. Furthermore, as an important advantage to be highlighted in relation to conventional multi-band BSF designs using filter banks, it utilizes less inverters and allows for theoretically arbitrary FBWs (>k_t^2) to be realized.

In order to illustrate the RF design principles of the multi-band AWLR-based BSF concept, Fig. 2 shows the power transmission response of an example third-order AWLR-based BSF that comprises three bands (N=3, K=3). The bands are shaped by AWRs that exhibit k_t^2=0.08% and respectively resonate at 415 MHz, 418 MHz, and 422 MHz. The illustrated responses were obtained with ideal linear simulations. In particular, Fig. 2(a) shows that the BW of each band can be independently controlled by readily altering the ratio of Z_B to Z_{AK} with wider BWs obtained for higher ratios. This feature can be realized in practice by incorporating variable reactive elements in Z_B or Z_{AK} as it will be discussed in the next section. It can be seen that the obtained FBWs can be designed to be wider than k_t^2 as opposed to conventional AWR-based architectures in which FBW is limited to 0.4-0.8k_t^2 [2]-[4]. Furthermore, Fig. 2(b) shows that the proposed architecture allows to control of the number of rejection bands by readily disconnecting the resonant branch of each band.

III. Experimental Validation

In order to validate the RF design principles of the multi-band AWLR-based BSF concept, a second-order dual-band prototype with N=K=2 that exhibits two rejection bands centered at 418 (band 1) and 434 (band 2) MHz was designed, manufactured, and measured. It was built on a Rogers 4003C dielectric substrate with: dielectric permittivity ε_r=3.38, dielectric thickness H=1.52 mm, loss tangent tan(δ_D)=0.0027, and 35-µm-thick Cu-cladding. The filter design was performed with post-layout electromagnetic (EM) simulations using the Advanced Design System (ADS) software package while taking into consideration the design guidelines in Section II. Commercially-available SAW resonators from Abracon and Epcos were employed. The circuit details of the manufactured prototype and its corresponding elements are shown in Fig. 3.

The RF performance of the filter was experimentally validated in terms of S-parameters with a Keysight N5224A PNA and is summarized in Figs. 4, 5. In particular, Fig. 4 shows a dual-band response with the following characteristics, low-band: stopband BW=0.49 MHz, FBW=1.54k_t^2, maximum in-bad isolation=22 dB, effective quality factor (Q_{eff})=3,500, upper-band: stopband BW=0.49 MHz, FBW=1.25k_t^2, maximum in-band isolation=23 dB, Q_{eff}=3,500. Furthermore, the passband insertion loss inbetween the rejection bands was measured around 1.6 dB. A comparison with the EM simulation

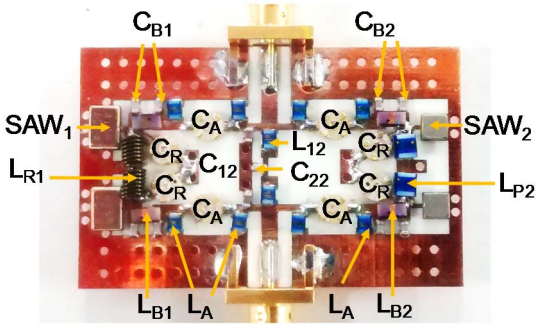

Fig. 3. Manufactured dual-band AWLR-based BSF. The impedance inverters $Z_{1,2}$, Z_{B1}, Z_{B2} were implemented with their first-order π-type low-pass circuit equivalent whereas Z_A was realized by its first-order π-type high-pass equivalent. The component values are summarized as follows: C_A= Johanson trimmer 2.5-10 pF, L_A=0805HQ-20N, C_{B1}= 251R14S0R6AV4T, L_{B1}= 1008HQ-68N, C_{B2}= 251R14S0R8BV4T, L_{B2}= 0805CS-680, L_{R1}= 1008CS-820, L_{R2}=0805CS-680, C_R= Johanson trimmer 1-5 pF, C_{12}= CL10C2R5CB8NNNC, C_{22}= 06031A5R0CAT2A, L_{12}= 0805HQ-12N, L_{P1}= 1111SQ-43N, L_{P2} =1008HQ-33N. SAW1: ASR418S2, and SAW2: R900.

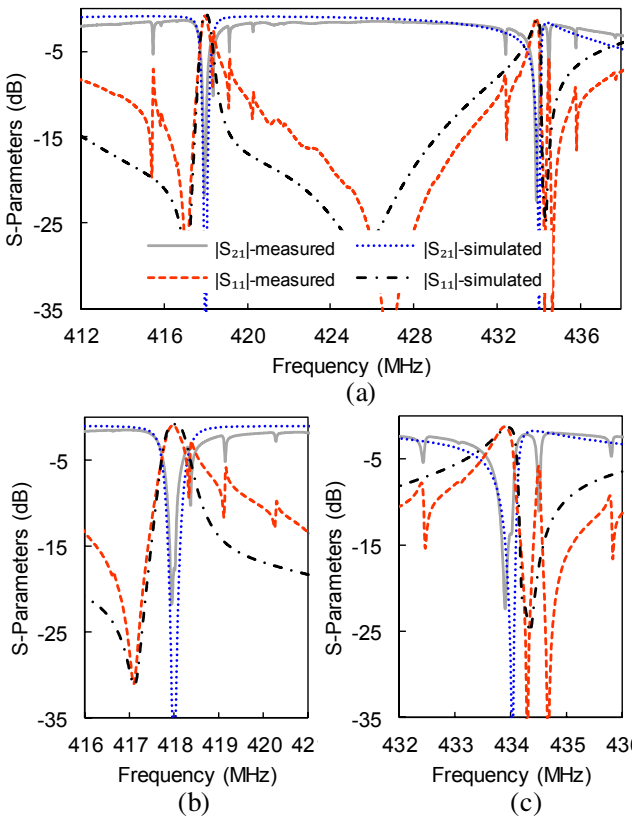

Fig. 4. RF measured and simulated S-Parameters of the second-order dual-band AWLR-based BSF prototype (N=K=2). (a) Wideband frequency response. (b) Detail of the low-frequency stopband. (c) Detail of the high-frequency stopband.

responses is also shown in the same figure which validates that the proposed multi-band AWLR-based BSF concept allows the realization of multiple rejection bands with FBW>k_t^2. The observed transmission peaks in the measured data are attributed to the multi-mode nature of the SAW resonator and are typically observed in all AWR-based filters [2]-[6].

The reconfiguration capabilities of the tunable multi-band BSF approach were experimentally validated by integrating variable trimmer capacitors in the Z_A inverters as well as at C_R in order to allow for symmetric/asymmetric BW tuning, Fig. 4. In particular, Fig. 5(a) shows continuous tuning of the upper band BW between 0.24-1.86 MHz (i.e, FBW=0.6-1.9k_t^2, tuning range=7.7:1) while the lower band remains static which proves the ability to independently control the BW of each band and in a wide range. While independent tuning of the lower band is not shown in this figure, it can be readily realized by tuning the capacitance of the Z_A inverters. Fig. 5(b) demonstrates the ability to simultaneously alter the BW of both bands. It is achieved by tuning the capacitance value of both Z_A inverters. Lastly, Fig. 5(c) demonstrates the ability to independently control the number of active rejection bands within a broad passband. It can be seen that each of the two bands can be independently switched-off (i.e., intrinsic RF switching-off) by altering the capacitance of the corresponding Z_A inverter. In

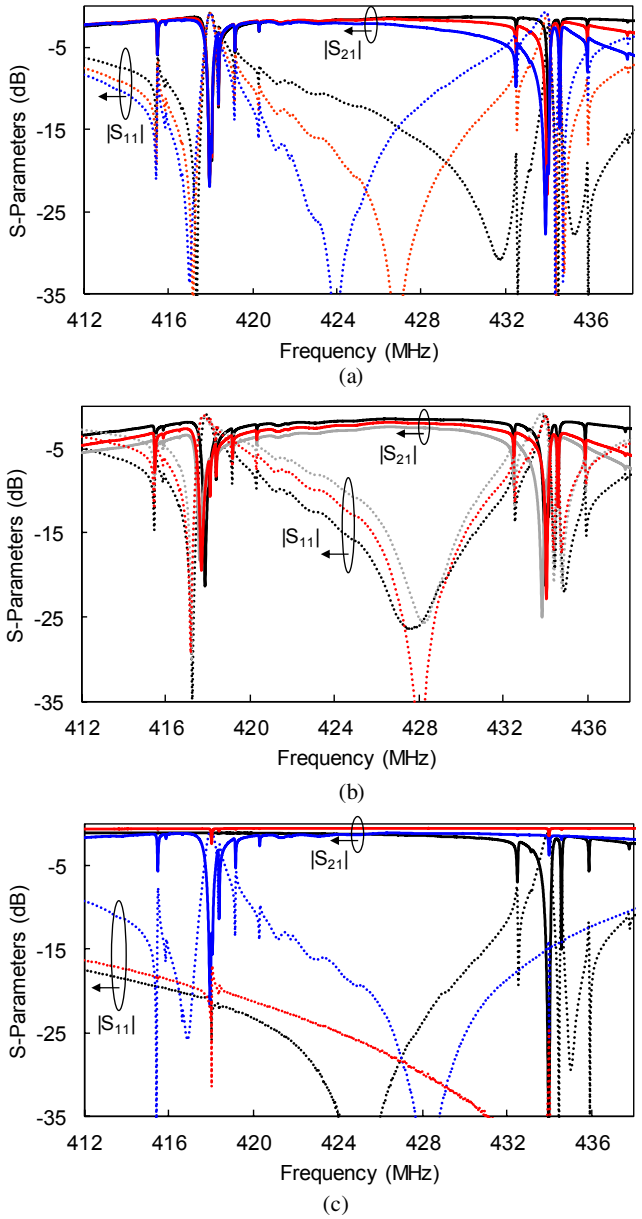

Fig. 5. RF measured S-Parameters of the dual-band AWLR-based BSF prototype (N=K=2) for various continuously tunable states. (a) Independent BW tuning of the upper band. (b) Symmetric BW tuning of both bands. (c) Intrinsic RF switching of each band and of both bands (all-pass response, red trace).

addition, by intrinsically switching-off both of the rejection bands, an all-pass state can be created.

IV. Conclusion

This manuscript reported on the design and implementation of a new class of multi-band AWLR-based BSFs with the following unique RF performance characteristics: i) multiple enhanced-FBW stopbands, ii) continuously-variable and independently-controlled stopband BWs (up to 7.7:1 tuning range), iii) intrinsically-switched rejection bands, and iv) an all-pass state. The proposed concept was experimentally validated at

UHF band through a second-order dual-band filter prototype that comprises of commercially-available SAW resonators.

ACKNOWLEDGMENT

This work has been supported in part by the National Science Foundation under Grant no. 1731956. The authors would like to thank Keysight for providing access to the software package Advanced Design System.

REFERENCES

[1] W. J. Chappell, E. J. Naglich, C. Maxey, and A. C. Guyette, "Putting the radio in "Software-defined radio": Hardware developments for adaptable RF systems," *Proc. IEEE*, vol. 102, no. 3, pp. 307–320, Mar. 2014.

[2] S. Gong and G. Piazza, "Design and analysis of Lithium-Niobate-based high electromechanical coupling RF-MEMS resonators for wideband filtering," *IEEE Trans. Microw. Theory Techn.*, vol. 61, no. 1, pp. 403–414, Jan. 2013.

[3] K. -W. Hsu, M. -C. Chang, and V. Lee, "Band-stop SAW notch filter using multiple resonators," in *Proc. Asia-Pacific Mircow. Conf.* Melbourne, VIC, Australia, Dec. 5-8, 2011, pp. 1114–1117.

[4] N. Hu, C. Zhou, W. Pang, and H. Zhang, "Temperature compensated band-pass and band-stop bulk-acoustic-wave filters solution reducing interference in wireless systems," in *Proc. Asia-Pacific Microw. Conf.* Melbourne, VIC, Australia, Dec. 5-8, 2011, pp. 1102–1105.

[5] D. Psychogiou, R. Gómez-García, and D. Peroulis, "High-*Q* bandstop filters exploiting acoustic-wave-lumped-element resonators (AWLRs)," *IEEE Trans. Circuits Syst. II, Exp. Briefs*, vol. 63, no. 1, pp. 79-83, Jan. 2016.

[6] D. Psychogiou, R. Gómez-García, and D. Peroulis, "Acoustic-wave-lumped-element resonator (AWLR) architectures for high-Q reflective bandstop filters," in *Proc. 45th European Microwave Conf. (EuMC)*, Paris, France, Sept. 7-10, 2015, pp. 422-425.

[7] D. Psychogiou, R. Gómez-García, and D. Peroulis, "Continuously-tunable-bandwidth acoustic-wave resonator-based bandstop filters and their multi-mode modeling," in *Proc. 46th European Microwave Conf. (EuMC)*, London, UK, Oct. 4-6, 2016, pp. 894-897.

[8] S. Doberstein, "Switchable low-loss SAW filter bands with MEMS switches," in *IEEE Ultrason. Symp.*, San Diego, CA, USA, Oct. 11–14, 2010, pp. 1294–1297.